



Experimental and theoretical investigations of structural and optical properties of CIGS thin films

M. Chandramohan^{a,*}, S. Velumani^b, T. Venkatachalam^{c,1}

^a Department of Physics, Park college of Engineering and Technology, Coimbatore-641 659, India

^b Centro de Investigacion y de Estudios Avanzados del I.P.N.(CINVESTAV), Av. Instituto Politecnico Nacional # 2508 Col. San Pedro Zacatenco 07360, Mexico D.F

^c Department of Physics, Coimbatore Institute of Technology, Coimbatore-14, India

ARTICLE INFO

Article history:

Received 30 August 2009

Received in revised form 13 March 2010

Accepted 17 March 2010

Keywords:

Chemical bath deposition

Thin Films

CIGS

Solar cells

Effective masses

Band gap

ABSTRACT

Experimental and theoretical studies of the structural and optical properties of Copper Indium Gallium diselenide thin films have been performed. Thin films of CIGS were deposited on glass substrates by chemical bath deposition. From the XRD results of the films, it is found that the films are of chalcopyrite type structure. The lattice parameter were determined as $a = 5.72 \text{ \AA}$ and $c = 11.462 \text{ \AA}$. The optical properties of the thin films were carried out with the help of spectrophotometer. First principles density functional theory calculations of the band structure, density of states and effective masses of electrons and holes of the CIGS crystals have been done by computer simulations. The experimental data and theoretically calculated data have demonstrated good agreement.

© 2010 Elsevier B.V. All rights reserved.

1. Introduction

At present thin films of copper indium diselenide (CIS) and copper indium gallium diselenide (CIGS) have received very good attention among the emerging materials for solar cell fabrication [1]. CIS and CIGS are direct band gap materials and have a large optical absorption coefficient; CIS and CIGS solar cell modules have shown long term stability [2]. Thin films of CIGS are considered as the most promising material for low cost and high efficiency, because of their high stability against photo degradation [3]. The best solar cells based on $\text{CuIn}_{1-x}\text{Ga}_x\text{Se}_2$ materials with $x < 0.3$ have reached efficiencies in the range of 20% [4–7]. The $\text{CuIn}_{1-x}\text{Ga}_x\text{Se}_2$ quaternary alloy is a semiconductor with the gap energies varying from 1 eV (for $x = 0$) to 1.7 eV (for $x = 1$); thus it allows tailoring of optical band gap for optimum solar cell conversion [7]. There is an increasing interest on fabrication technology and properties of $\text{CuIn}_{1-x}\text{Ga}_x\text{Se}_2$ thin films. CIGS thin films have been deposited using various techniques including physical evaporation [8–10], rapid thermal process [11], selenization of sequentially stacked precursors [12,13]. All these vacuum deposition techniques are carried out to be heavy and expensive. It is found that chemical bath deposition

technique is low cost, potentially suitable to obtain good quality, large area CIGS precursor films and they are suitable for growing large area thin films economically. A better understanding of the quaternary formation processes is essential for optimizing these films for solar cell fabrication. We present the results of investigation of the structural and optical properties of chemical bath deposited $\text{CuIn}_{1-x}\text{Ga}_x\text{Se}_2$ thin films and also the simulation results of the chalcopyrite CIGS structure.

2. Experimental details

2.1. Deposition of thin films

Cu, In, Ga, and Se atoms are co-deposited from the solution onto the well-cleaned substrates with the help of their ions in reaction mixture. The reaction mixture used for preparing CIGS thin films consists of CuCl_2 , LiCl , GaCl_3 , H_2SeO_3 , and InCl_3 substances of analytical grade chemicals (99.99% Sigma Aldrich) [14]. The mixture was prepared by taking each 10 ml of above solutions in 100 ml beaker. The pH value of mixture was measured with the help of digital pH meter and it was found to be 2 ± 0.05 . Two well-cleaned glass plates ($37.5 \text{ mm} \times 12.5 \text{ mm} \times 1 \text{ mm}$) were suspended vertically with the help of substrate holder and dipped into the beaker containing the reaction mixture. The beaker containing the reaction mixture and glass substrates was placed in water bath, was stirred with the help of magnetic stirrer as shown in Fig. 1. The deposition bath turned pure white and then to colorless as the time

* Corresponding author. Tel.: +91 0421 2334899; fax: +91 0421 2334453.

E-mail addresses: chandramohan59@yahoo.co.in (M. Chandramohan), vels64@yahoo.com (S. Velumani), atvenkatachalam@yahoo.com (T. Venkatachalam).

¹ Tel.: +9104222574071; Fax: +91-422-2575020.

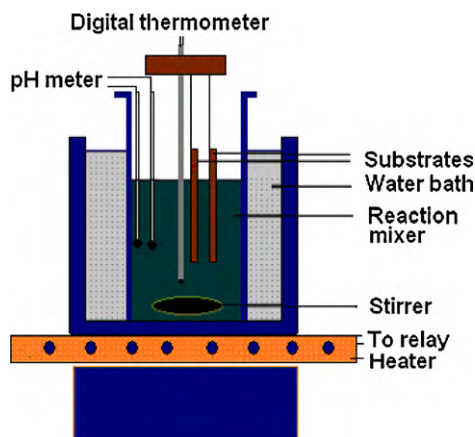


Fig. 1. Schematic diagram of chemical bath.

progress. The deposition was carried-out at two different temperatures (300 K, and 323 K) by taking two different time of deposition (60 min and 120 min). The mixture with glass substrates was kept at one particular temperature and stirred continuously, while stirring the solution; the substrates were taken out at the intervals of 60 minutes. The glass plates were dried in open air in order to evaporate the moisture content. Two representative films from each deposition temperatures 300 K and 323 K are identified and labeled as film 1 and film 2 for the characterization.

2.2. Characterization of thin films

The structural analysis of the films is carried out using a computer controlled X-ray diffractometer system model JDX 8030 with Ni filter and Cu K α radiation. The scanning is carried out using θ - 2θ scan coupling mode the ratings being 40 kV, 20 mA. The crystalline sizes (D) are calculated using the Scherrer's formula from the full width at half maximum (β) using the relation $D = 0.94\lambda/\beta \cos \theta$. The strain (ϵ) is calculated from the slope of $\beta \cos \theta$ versus $\sin^2 \theta$ plot using the relation $\beta = \lambda/D \cos \theta - \epsilon \tan \theta$. The dislocation density (δ) is evaluated from the relation $\delta = 1/D^2$. The width of the peaks decreases as the deposition temperature increases. This could be due to reduced strain within the film or an increase in grain size indicating a better crystalline perfection. The lattice parameters (a and c) of the crystal are determined by using the relation

$a^2/(h^2 + k^2) + c^2/l^2 = 1/d^2$, where (hkl) is the miller indices of the peaks. The particle size, lattice parameter, strain, lattice spacing and dislocation density values for the various films have been calculated. Micro structural investigations of thin films on glass substrate are carried out using Scanning Electron Micrograph (SEM JOEL). Compositions of the films are determined by EDAX measurements (JOEL). Thicknesses of all the films are measured by using multiple beam interferometer technique. The optical studies are made on the films deposited on glass substrates in the wavelength range from 190 to 2500 nm at room temperature by using spectrophotometer (JASCO-370 V).

2.3. CIGS simulation

The calculations were performed within the framework of the density functional theory (DFT) [15]. The exchange correlation term was treated by using the functional of LDA - CA PZ [16] and GGA-PW91 [17,18]. The ultra-soft pseudo-potential was applied to describe the electron-ion interaction. A plane wave basis set with a 290 eV energy cut-off was used to expand the electronic wave functions. Reciprocal space integration was performed by k-point sampling with sets of special points obtained by using the standard special k points technique of the Monkhorst and Pack. In our case (i.e. for Chalcopyrite CIGS) a $4 \times 4 \times 2$ MP meshes were used, yielding ten k points in the irreducible wedge of the Brillouin zone. CIGS chalcopyrite structure belongs to P65 symmetry group, which displays only identity and inversions operations.

3. Results and discussion

3.1. Structure and composition of thin films

All the films deposited on well cleaned glass substrates are smooth, uniform, adherent and transparent in color. The transparency decreases with increase in thickness of the thin films. Fig. 2 shows XRD graphs of the thin films (deposition temperatures 300 K and 323 K) of thicknesses 1500 nm, and 3700 nm respectively. The predominant peaks in XRD graph of CIGS thin films could be probably associated with (101), (112), (103), (211), and (105) reflections of the chalcopyrite structure. The peak intensities of all the film increases with increase in deposition temperature, it is due to increase in the crystalline nature of the film. The lattice parameters, particle sizes, strain and dislocation densities of thin films

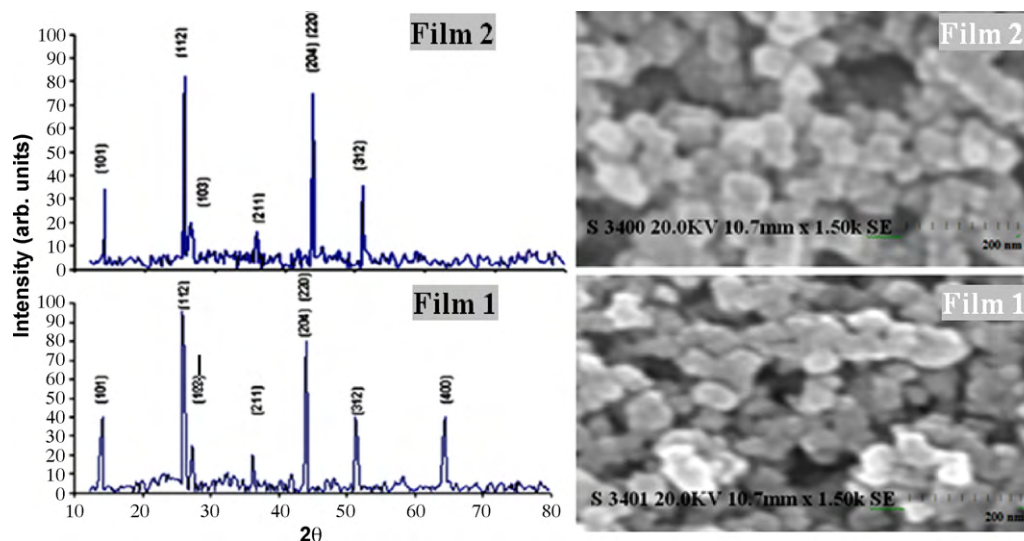


Fig. 2. X-ray diffraction pattern and SEM images of CIGS thin films.

Table 1
XRD results of CIGS thin films.

Film#	Lattice parameter (Å)		Particle size (D) (nm)	Strain (ϵ) ($\times 10^{-4}$ lines $^{-2}$ m 4)	Dislocation density (δ) ($\times 10^{12}$ lines m $^{-2}$)
	a	c			
1	5.7236	11.4472	397	1.708	6.344
2	5.7332	11.4664	445	0.409	5.049

Table 2
Results of EDAX studies.

Film #	Cu (%)	In (%)	Ga (%)	Se (%)	Molecular formula
1	21.04	9.13	17.54	52.29	CuIn _{0.24} Ga _{0.76} Se ₂
2	20.97	9.85%	17.05	52.13	CuIn _{0.26} Ga _{0.74} Se ₂

deposited are given in Table 1. It is found that the size of the particle increases with the bath temperature in all the films. These results are in agreement with the SEM results. The compositions of the films are identified from the EDAX measurements and their data are tabulated (Table 2). The particle sizes in SEM micrograph of all the alloys are measured and the mean values of the particle sizes are found to be 397 nm (film 1), and 445 nm (film 2) which are very close to the XRD results.

3.2. Optical studies of thin films

The optical transmittance spectra of thin films are as shown in Fig. 3. The insets in the graph shows the corresponding plot of $(\alpha h\nu)^2$ versus $h\nu$ and the extrapolation of the linear portion to the abscissa are the band energy gap of the film. The absorption coefficient α is estimated from the optical transmittance spectra using the relation $\alpha = 2.303 \log(1/T)/t$ where T is the transmittance (in %) and t is the thickness of the film. All such graph satisfies the condition for a direct transition in the excitation process i.e. $\alpha = (E_v - E_i)^{1/2}$ for allowed direct transition, where E_v is the top of the valence band and E_i is energy of the initial state from which the transition is made. All the films exhibit direct band gap structure and their band gap values are found to be 1.15 eV (film 1), and 1.1 eV (film 2) [18,19]. Hence as starting point we have computed the structural and band energy gap of the chalcopyrite structure (Fig. 4) of Cu(In_{0.25}Ga_{0.75})Se₂ using self consistently.

3.3. *ab initio* studies of CIGS structure

We performed the *ab initio* band calculations for the structure with both local density approximation and generalized gradient approximation schemes. The equilibrium lattice parameters were comparable with the experimental data. The computed band structure of the compound using both LDA and GGA schemes indicate a direct band gap located at the gamma point. It is clearly that

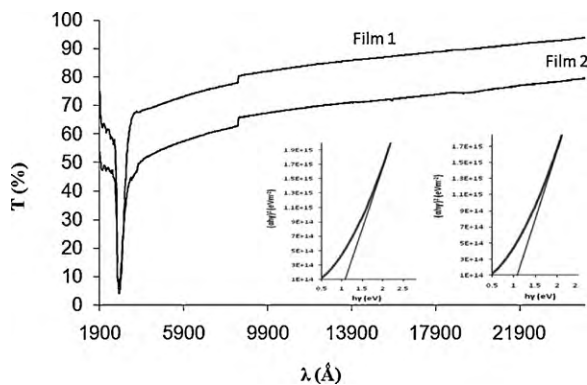


Fig. 3. Transmittance spectra and dependence of $(\alpha h\nu)^2$ on photon energy for CIGS thin films.

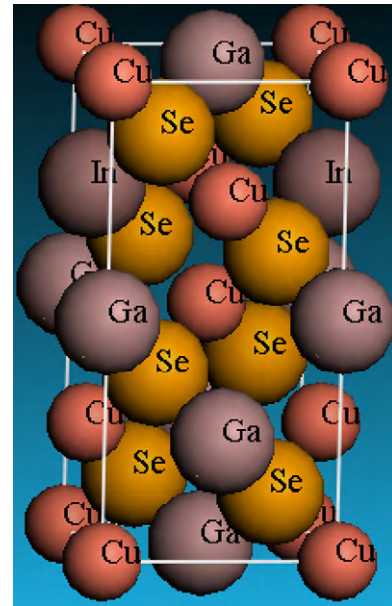


Fig. 4. Chalcopyrite structure of CuIn_{0.25}Ga_{0.75}Se₂.

the band gap values given by LDA and GGA are in good agreement with the experiments. Effective masses of electrons and holes are important parameters describing the most carrier transport properties in the compound. The effective masses of the electrons and holes near the gamma valley are calculated from the equation $1/m^* = 4\pi^2/h^2 (d^2E/dk^2)$. The effective masses of the electrons and holes are 0.089 m_e and 0.693 m_e .

4. Conclusions

Good quality thin films of the CIGS have been prepared by a chemical bath deposition method with two different bath temperatures and two different deposition times. X-ray analysis revealed that the films are crystalline in nature with chalcopyrite phase (lattice parameters nearly $a=5.72$ Å and $c=11.462$ Å) and their molecular formulae are CuIn_{0.24}Ga_{0.76}Se₂ and CuIn_{0.26}Ga_{0.74}Se₂. Optical studies revealed that the thin fundamental absorption edge arises at 1.15 eV (film 1) and 1.1 eV (film 2). The band gaps are due to the direct electronic transition. The first principles pseudo-potential method is used to investigate the structural properties and stability of the compounds CuIn_{0.24}Ga_{0.76}Se₂ and CuIn_{0.26}Ga_{0.74}Se₂. The calculated energy band gap values of experimental and simulated CIGS were found to be in good agreement to each other as well as with those reported in the literature. The reported results give an indication that the deposited layers may find applications in the fabrication of thin film solar cells and photo-detector.

Acknowledgments

We are grateful to Dr. Hongbo Liu (Mexico) for the discussion and computational works in this paper.

References

- [1] R. Ugarte, R. Schrebler, R. Cordova, E.A. Dalchiale, H. Gomez, *Thin Solid Films* 340 (1999) 117–124.
- [2] A.M. Fernandez, R.N. Battacharaya, *Thin Solid Films* 474 (2005) 10–13.
- [3] R.N. Bhattacharya, W. Batchelor, J.E. Granata, F. Hasoon, H. Wiesner, K. Ramanathan, J. Keane, R.N. Nou, *Solar Energy Materials and Solar Cells* 55 (1998) 83–94.
- [4] K. Bouabid, A. Ihlal, A. Manar, A. Outzourhit, E.L. Ameziane, *Thin Solid Films* 488 (2005) 62–67.
- [5] T. Wada, Y. Hashimoto, S. Nishiwaki, T. Satoh, S. Hayashi, T. Negami, H. Miyake, *Solar Energy Materials & Solar Cells* 67 (2001) 305–310.
- [6] M.A. Contreras, B. Eggas, K. Ramanathan, J. Hiltner, A. Swartzlander, F. Hasoon, R. Noufi, *Prog. Photovoltaics* 7 (1999) 311.
- [7] K. Ramanathan, G. Teeter, J.C. Keane, R. Noufi, *Thin Solid Films* 480 (2005) 499.
- [8] V. Nadenau, D. Braunger, D. Hariskos, M. Kaiser, Ch. Koble, A. Oberacker, M. Ruckh, U. Ruhle, R. Schaffler, D. Schmid, T. Walter, S. Zweigart, H.W. Schock, *Prog. Photovolt* 3 (1995) 363.
- [9] M.A. Contreras, J.R. Tuttle, A.M. Gabor, A.L. Tennant, K.R. Ramanathan, S. Asher, A. Franz, J. Keane, L. Wang, R. Noufi, *Prog. Photovolt* 3 (1995) 383.
- [10] M.A. Contreras, J.R. Tuttle, A.M. Gabor, A.L. Tennant, K.R. Ramanathan, S. Asher, A. Franz, J. Keane, L. Wang, R. Noufi, *Sol. Energy Mater. Sol. Cells* 41/42 (1996) 231.
- [11] M. Wagner, I. Dirstorfer, M.M. Hofmann, M.D. Lampert, f. Karg, B.K. Meyer, *Phys. Status Solidi, A Appl. Res* 167 (1998) 131.
- [12] S. Nakagawa, H. Ishihara, N. Mochizuki, T. Kamiya, K. Toyoda, T. Ikeya, K. Sato, M. Ishida, 14th European Photovoltaic Solar energy conf. Barcelona, 1997, p.1216.
- [13] C. Guillen, J. Herrero, *Thin Solid Films* 323 (1998) 93–98.
- [14] M. Dhanam, R. Balasundaraprabhu, S. Jayakumar, P. Gopalakrishnan, M.D. Kannan, *Phys. Stat. Sol. (a)* 1 (2002) 149–160.
- [15] M.D. Segall, P.J.D. Lindan, M.J. Probert, C.J. Pickard, P.J. Hasnip, S.J. Clark, M.C. Payne, *J. Phys.: Cond. Matt.* 14 (11) (2002) 2717–2743.
- [16] D.M. Ceperley, B.J. Alder, *Phys. Rev. Lett* 45 (1980) 566.
- [17] J.P. Perdew, A. Zunger, *Phys. Rev. B* 23 (1981) 5048.
- [18] J.P. Perdew, S. Burke, M.E. Ernzerhof, *Phys. Rev. Lett* 77 (1996) 3865.
- [19] M. Venkatachalam, M.D. Kannan, S. Jayakumar, R. Balasundaraprabhu, N. Muthukumarasamy, A.K. Nandakumar, *Solar Energy Materials & Solar Cells* 92 (2008) 517–575.